Directed motion of C_{60} on a graphene sheet subjected to a temperature gradient

A. Lohrasebi,[1] M. Neek-Amal,[2] and M. R. Ejtehadi[3]
[1]*Department of Physics, University of Isfehan, Isfehan, Iran, and School of Nano Science, Institute for Research in Fundamental Sciences (IPM), Iran*
[2]*Shahid Rajaee Teacher Training University, Lavizan, Tehran 16788, Iran*
[3]*Department of Physics, Sharif University of Technology, P.O. Box 1155-9161, Tehran, Iran*
(Received 22 May 2010; revised manuscript received 20 December 2010; published 29 April 2011)

Nonequilibrium molecular dynamics simulations are used to study the motion of a C_{60} molecule on a graphene sheet subjected to a temperature gradient. The C_{60} molecule is actuated and moves along the system while it just randomly dances along the perpendicular direction. Increasing the temperature gradient increases the directed velocity of C_{60}. It is found that the free energy decreases as the C_{60} molecule moves toward the cold end. The driving mechanism based on the temperature gradient suggests the construction of nanoscale graphene-based motors.

DOI: 10.1103/PhysRevE.83.042601 PACS number(s): 68.43.−h, 65.80.Ck

I. INTRODUCTION

Since graphene was discovered [1], many properties of this two-dimensional material have been studied both experimentally [2] and theoretically [3,4]. In recent experimental research the dynamic of light atoms deposited on a single-layer graphene has been studied by means of the transmission electron microscopy technique [5]. The two-dimensional structure of graphene suggests the possibility of motion with just two degrees of freedom. The free-energy surface for a particle moving above a graphene sheet explains different motion-related phenomena at the nanoscale as well as the various directed motions on the carbon nanotube-based motors [6,7].

A net motion can be obtained from a nanoscale system subjected to a thermal gradient [8,9]. Recently the motion of an experimentally designed nanoscale motor consisting of a capsule-like carbon nanotube inside a host carbon nanotube has been explained successfully with molecular dynamics (MD) simulations [10]. The capsule travels back and forth between both ends of the host carbon nanotube along the axial direction. Barreiro *et al.* have designed an artificial nanofabricated motor in which one short carbon nanotube travels relative to another coaxial carbon nanotube [7]. This motion is actuated by a thermal gradient as high as 1 K nm^{-1} applied to the ends of the coaxial carbon nanotubes.

Since graphene has a very high thermal conductivity (3000–5000 W K^{-1} m^{-1} [11,12]), as high as diamond and carbon nanotubes [13–16], it is a good candidate for heat-transferring designs in nano-electromechanical systems. Because of strong covalent bonds in graphene, thermal lattice conduction dominates the electrons' contribution [11]. Recently Yang *et al.* [17] have studied the thermal conductivity and thermal rectification of trapezoidal and rectangular graphene nanoribbons and found a significant thermal rectification effect in asymmetric graphene ribbons [17].

Here we study the motion of a nanoscale object, e.g., C_{60}, on a graphene sheet, in the presence of a temperature gradient. We show that the graphene is a good two-dimensional substrate for thermal actuation due to its high thermal conductivity; however, as is expected, in the absence of a thermal gradient, the C_{60} molecule randomly diffuses on the graphene sheet [6]. The average velocity along the temperature gradient direction and the free-energy change throughout the system are calculated.

This paper is organized as follows. In Sec. II we will introduce the atomistic model and the simulation method. Section III contains the main results, including those for the produced temperature gradient, the trajectory of the C_{60} molecule over the graphene sheet, and the free-energy change. A brief summary and conclusions are included in Sec. IV.

II. THE MODEL AND METHOD

The system was composed of a graphene sheet as a substrate, with dimensions $L_x \times L_y = 70\times5$ nm^2 and a C_{60} molecule above the sheet. The graphene sheet with $N = 14\,400$ carbon atoms was divided into 12 equal rectangular segments. Each segment with $N_l = 1200$ carbon atoms was arranged in 40 atomic rows (along the armchair or x direction). Each row has 30 atoms, which were arranged along a zigzag direction. The system was equilibrated for 300 ps at $T = 300$ K before the temperature gradient was applied. Once the system was equilibrated, the first (hot spot) and last (cold end) segments of the graphene sheet were kept at T_h and T_c, respectively. A temperature gradient between the two ends was then produced, i.e., $(T_h - T_c)/L_x$ (top panel of Fig. 1). To make the model more efficient and prevent crumpling [see Fig. 2(a)] of the ends, we fixed the z components of the first atomic row in the first segment and the last row of the last segment [see Fig. 2(b)].

We carried out MD simulations employing two types of the interatomic potentials: (1) the covalent bonds between the carbon atoms in the graphene sheet and in the C_{60} molecule are described by Brenner potential [18] and (2) the nonbonded Van der Waals interactions between the graphene atoms and those of the C_{60} molecule. Brenner potential has been parameterized to model sp^2 covalent bonds in the graphene, carbon nanotube, and C_{60} structures. For the nonbonded potential a Lennard-Jones (LJ) potential gives reasonable results [19]. Here we choose the LJ parameters as $\epsilon = 2.413$ meV and $\sigma = 3.4$ Å [20], which represent the depth and range of the LJ potential energy, respectively. Note that the LJ potential is a simple and commonly used potential for modeling the interaction between

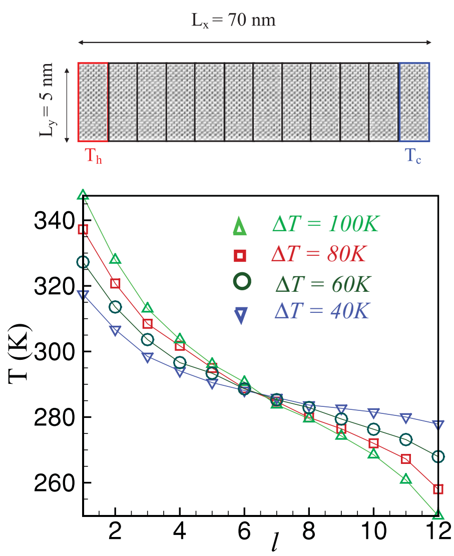

FIG. 1. (Color online) Top: The model, which shows an applied temperature gradient along the x direction. Bottom: Produced four temperature gradients after 450 ps of a nonequilibrium molecular dynamics simulation. Delta symbols are related to $\Delta T = 100$ K, square symbols $\Delta T = 80$ K, circle symbols $\Delta T = 60$ K, and gradient symbols $\Delta T = 40$ K.

carbon nanostructures [21,22]. The equations of motion were integrated using a velocity-Verlet algorithm with a time step $\Delta t = 0.5$ fs. The temperature of the hot end (T_h) and the cold end (T_c) were held constant by a Nosé-Hoover thermostat. The temperature of the inner segments were not controlled by the thermostat. The periodic boundary condition was applied only in the y direction. Due to the applied temperature gradient, the system can no longer be described by equilibrium methods, and we shall thus employ nonequilibrium molecular dynamics simulations. A temperature gradient were produced across the system over 450 ps, and a stationary state was established. The C_{60} molecule was put above the second segment at $z_{\rm cm} = 8$ Å (here the index cm refers to the center of mass). During the production runs of 750 ps both the x and y positions of the center of mass of the C_{60} molecule were recorded. Moreover the temperature of each segment was calculated by measuring the total kinetic energy of that segment. In our simulations a typical value for the relative standard deviation of the total energy of the extended system is about 3.5×10^{-5}. A full simulation run takes about 50 h CPU time on a 3.2 GHz Pentium IV processor with 4 GB RAM.

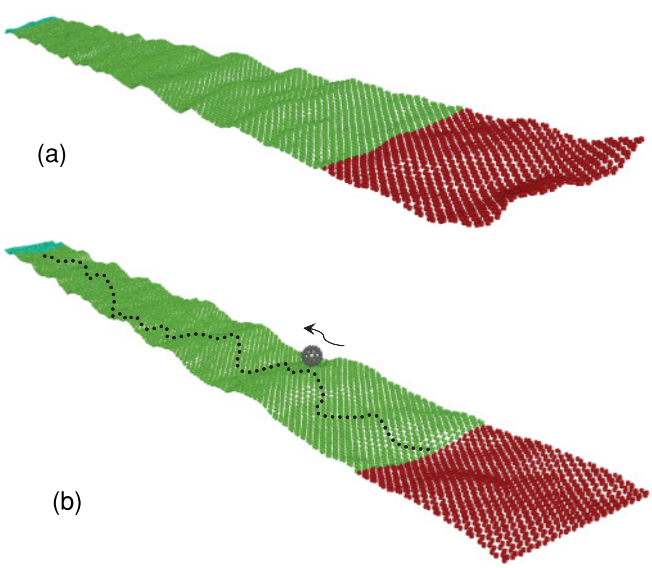

FIG. 2. (Color online) (a) A snapshot of an unconstrained system shows the effect of the ends crumpling. (b) Fixing z components of the atoms at the first and last rows (see the text) prevents the crumpling. The black dots show a typical trajectory of the motion of a C_{60} molecule over the graphene sheet from the hot spot toward the cold spot.

In order to compute the change in the free energy, one can employ the commonly used thermodynamic integration and perturbation methods [23]. A good estimation for the absolute value of the free energy requires sampling the whole phase space, which is not feasible. Jarzynski's method removes this difficulty for nonequilibrium simulations [24]. There is an equality between the change of the free energy F and the work W applied on the system (here the C_{60} molecule) [24]

$$\Delta F = -\beta^{-1} \ln \overline{\exp(-\beta W)}, \qquad (1)$$

where $\beta = 1/k_B T$ (T is the temperature in each segment), and the average is taken over different configurations with different initial conditions. In fact, Eq. (1) connects the change of the free energy (between two equilibrium state) and the applied work on the system in a nonequilibrium process.

III. RESULTS AND DISCUSSION

A. Producing temperature gradients

The temperature profiles for different temperature gradients with $\Delta T = 40, 60, 80$, and 100 K are shown in Fig. 1 (bottom panel). In this figure, the local temperatures of each segment, which were obtained by averaging over 500 data, are indicated by symbols. Corresponding error bars indicate the statistical errors and are in the range 4–6 K. Notice that the temperature profiles are nonlinear, which is a commonly observed behavior in a nonequilibrium molecular dynamics simulation of thermal conductivity [14–16]. It is a consequence of the strong phonon scattering caused by the heat source or heat sink and can be explained by partly diffusive and partly ballistic energy transport along the system [14,25]. Also, ripples in the graphene [Fig. 2(b)] are the other important source for phonon scattering [26,27]. Therefore, these mechanisms cause a nonlinear temperature profile in the middle segments.

B. Trajectory in the x-y plane

The graphene ribbon is a two-dimensional way for the motion of the C_{60} molecule along it. C_{60} attempts to find its equilibrium state and looks for the local minimum of the free energy. In other words, in the presence of a temperature gradient, the phonon waves created in the hot spot travel through the system, interact, and transfer momentum to the C_{60} molecule, which results a net motion [7]. The time series for the x and y coordinates, separately, are shown in Figs. 3(a) and 3(b). The trajectories of the six C_{60} molecules (from the six different simulations) in x-y plane over a time interval of

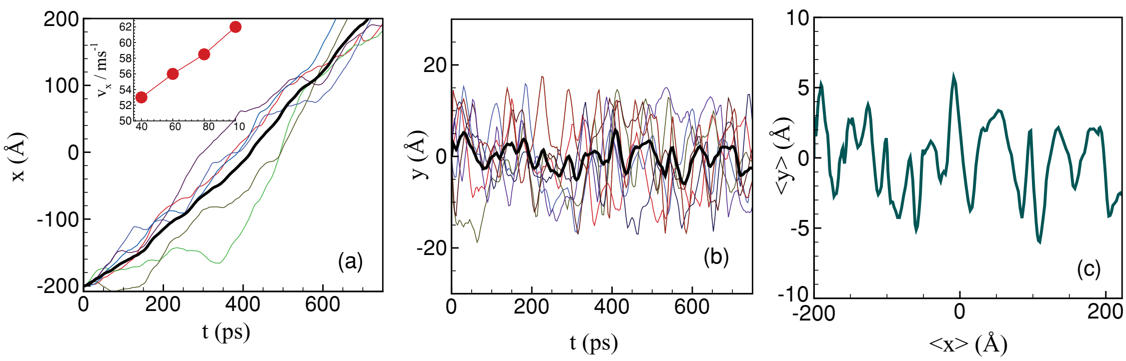

FIG. 3. (Color online) (a, b) Time series of x and y components of the center of mass of a C_{60} molecule over a monolayer graphene subjected to a temperature gradient. Thick curves show the average curves. The inset shows the variation of the velocity versus temperature gradient. (c) The trajectory of the motion of a C_{60} molecule (in a x-y plane) moving over the monolayer graphene, averaged over six simulations with different initial conditions.

750 ps are depicted in Fig. 3(c). In all three cases the thick curve is the average of the six others.

The motion along the x direction is almost a linear uniform motion with velocities $v_x = 53, 56, 59$, and 63 m/s for $\Delta T = 40, 60, 80, 100$ K, respectively [see inset of Fig. 3(a)]. There are two computational methods that can be used to show that the motion along the y direction is diffusive [Fig. 3(c)]. First, one can use the Einstein relation to find the diffusion constant D_y by measuring the slope of the mean square displacement (MSD) of the y components of the position, i.e., $\langle [y(t) - y(0)]^2 \rangle$. To show that the motion along the y direction is driftless, we look at the MSD of the y component of the position of the C_{60} molecule. For a driftless motion the MSD should grow linearly with time, i.e., $< [y(t) - y(0)]^2 >= 2D_y t$. We depict the MSD in Fig. 4 for a long time simulation. As we see from this figure the slope of the MSD is almost one (after equilibration), which is a signature of diffusive regime. Alternatively one can use the Green-Kubo relation, which makes use of the velocity autocovariance function (VACF). More specifically, one can take the integral over the autocovariance of the y components of the position of the velocity of C_{60} as $D_y = \int_0^\infty \langle v_y(0) v_y(\tau) \rangle \, d\tau$, which gives the diffusion constant of random-walk motion along the y axis. The inset of Fig. 4 shows the VACF versus time. We have tested both methods in order to compute D_y. The result for the diffusion constant is about 4×10^{-9} m^2/s.

The directed motion resulted from the temperature gradient along the graphene sheet provides a nanoscale motor for

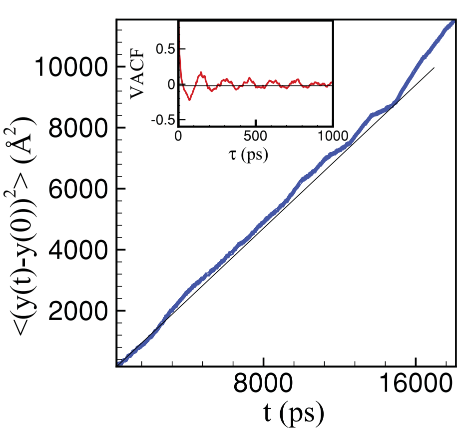

FIG. 4. (Color online) Mean square displacement for the y component of the center of mass of a C_{60} molecule over the graphene. The inset shows the velocity autocorrelation function for the y component of the motion as a function of time.

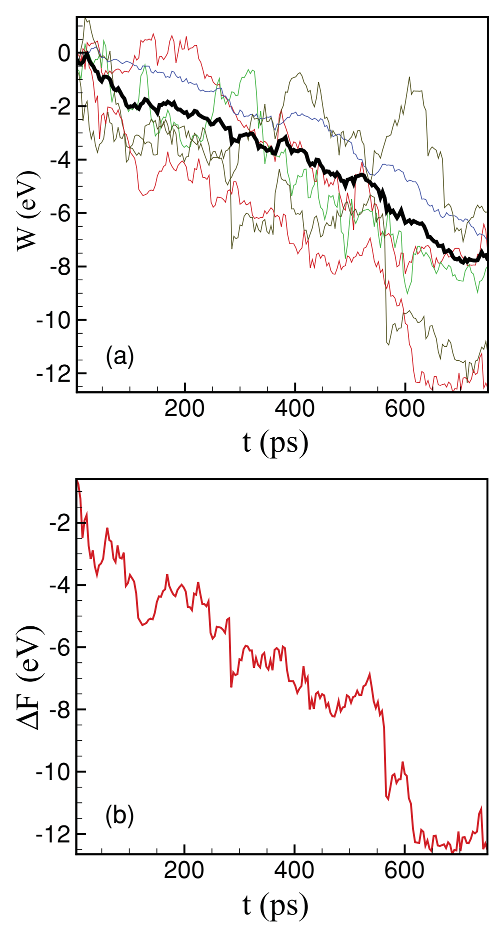

FIG. 5. (Color online) (a) Total work performed on C_{60} molecules and (b) the change of free-energy during C_{60} motion from the hot end to the cold end. The thick curve is the average over six simulations with different initial conditions.

the material transferring. Notice that in the absence of a temperature gradient, when the system is equilibrated at $T = 300$ K, we found a diffusive motion on the graphene sheet [6].

C. Free-energy reduction

Figures 5(a) and 5(b) show the variation of the total work and the changes in the free energy with time, respectively. The C_{60} loses on average almost 12 eV of free energy after 750 ps during the motion toward the cooler region. Note that here the condition $\overline{W} > \Delta F$ is always satisfied, which is a well-known criterion for a nonequilibrium (irreversible) thermodynamics evolution [24]. This method for calculating the change of the free energy is a well-known method in computational soft condensed matter [28], but it turns out to be useful also for studying various physical properties of graphene, particularly investigating the stability of new designs for nanoscale molecular devices as studied here.

IV. CONCLUSIONS

In summary, C_{60} moves directly toward the cold end of the graphene sheet when a temperature gradient is applied along armchair direction. It is found that the lateral motion (along the zigzag direction) is a diffusive motion. The reduction of the free energy of the system along the molecule motion is indicative of the drifted motion. Comparing the free-energy difference with the work performed on C_{60} shows that the process is indeed thermodynamically irreversible. The proposed mechanism for driving nanoparticles on a graphene sheet may be used in the design of novel nanoscale motors.

ACKNOWLEDGMENT

We gratefully acknowledge valuable comments from Hamid Reza Sepangi and Ali Naji.

[1] K. S. Novoselov, A. K. Geim, S. V. Morozov, D. Jiang, Y. Zhang, S. V. Dubonos, I. V. Grigorieva, and A. A. Firsov, Science **306**, 666 (2004).

[2] A. K. Geim and K. S. Novoselov, Nat. Mater. **6**, 183 (2007).

[3] A. K. Geim and A. H. MacDonald, Phys. Today **60**, 35 (2007).

[4] A. H. Castro Neto, F. Guinea, N. M. Peres, K. S. Novoselov, and A. K. Geim, Rev. Mod. Phys. **81**, 109 (2009).

[5] J. C. Meyer, C. O. Girit, M. F. Crommie, and A. Zettl, Nature (London) **454**, 319 (2008).

[6] M. Neek-Amal, N. Abedpour, S. N. Rasuli, A. Naji, and M. R. Ejtehadi, Phys. Rev. E **82**, 051605 (2010).

[7] A. Barreiro, R. Rurali, E. R. Hernandez, J. Moser, T. Pichler, L. Forro, and A. Bachtold, Science **320**, 775 (2008).

[8] P. A. E. Schoen, J. H. Walther, S. Arcidiacono, D. Poulikakos, and P. Koumoutsakos, Nano Lett. **6**, 1910 (2006).

[9] P. A. E. Schoen, J. H. Walther, D. Poulikakos, and P. Koumoutsakos, Appl. Phys. Lett. **90**, 253116 (2007).

[10] H. Somada, K. Hirahara, S. Akita, and Y. Nakayama, Nano Lett. **9**, 62 (2009).

[11] A. A. Balandin, S. Ghosh, W. Bao, I. Calizo, D. Teweldebrhan, F. Miao, and C. N. Lau, Nano Lett. **8**, 902 (2008).

[12] S. Ghosh, I. Calizo, D. Teweldebrhan, E. P. Pokatilov, D. L. Nika, A. A. Balandin, W. Bao, F. Miao, and C. N. Lau, Appl. Phys. Lett. **92**, 151911 (2008).

[13] S. Berber, Y-K. Kwon, and D. Tomanek, Phys. Rev. Lett. **84**, 4613 (2000).

[14] P. K. Schelling, S. R. Phillpot, and P. Keblinski, Phys. Rev. B **65**, 144306 (2002).

[15] E. Gonzalez Noya, D. Srivastava, Leonid A. Chernozatonskii, and M. Menon, Phys. Rev. B **70**, 115416 (2004).

[16] M. A. Osman and D. Srivastava, Nanotechnology **12**, 21 (2001).

[17] N. Yang, G. Zhang, and B. Li, Appl. Phys. Lett. **95**, 033107 (2009).

[18] D. W. Brenner, Phys. Rev. B **42**, 9458 (1990).

[19] H. Ulbricht, G. Moos, and T. Hertel, Phys. Rev. Lett. **90**, 095501 (2003).

[20] G. Stan, M. J. Bojan, S. Curtarolo, S. M. Gatica, and M. W. Cole, Phys. Rev. B **62**, 2173 (2000).

[21] P. A. Gravil, M. Devel, Ph. Lambin, X. Bouju, C. Girard, and A. A. Lucas, Phys. Rev. B **53**, 1622 (1996).

[22] A. N. Kolmogorov and V. H. Crespi, Phys. Rev. Lett. **85**, 4727 (2000).

[23] F. Colonna, J. H. Los, A. Fasolino, and E. J. Meijer, Phys. Rev. B **80**, 134103 (2009).

[24] C. Jarzynski, Phys. Rev. Lett. **78**, 2690 (1997).

[25] C. Oligschleger and J. C. Schon, Phys. Rev. B **59**, 4125 (1999).

[26] K. V. Zakharchenko, M. I. Katsnelson, and A. Fasolino, Phys. Rev. Lett. **102**, 046808 (2009).

[27] N. Abedpour, M. Neek-Amal, R. Asgari, F. Shahbazi, N. Nafari, and M. R. Tabar, Phys. Rev. B **76**, 195407 (2007).

[28] H. Xiong, A. Crespo1, M. Marti, D. Estrin, and A. E. Roitberg, Theor. Chem. Acc. **116**, 338 (2002).